Electroweak quantum chemistry for nuclear-magnetic-resonance-shielding constants: Impact of electron correlation

Guido Laubender and Robert Berger*

Frankfurt Institute for Advanced Studies, Johann Wolfgang Goethe-University, Max-von-Laue-Straße 1, D-60438 Frankfurt/Main, Germany

(Received 20 April 2006; published 14 September 2006)

One promising route towards the first experimental verification of parity violation (PV) in chiral molecular systems is the detection of line splittings between nuclear magnetic resonance (NMR) spectra of enantiomers. Those numerical methods which can be systematically refined and allow for an accurate and reliable prediction of molecular PV effects will play a crucial role for the preparation and interpretation of such experiments. In this work the *ab initio* calculation of isotropic parity-violating NMR-shielding constants (σ^{PV}) within coupled cluster and multiconfiguration linear response approaches to electroweak quantum chemistry is reported and the results are compared to data obtained at the uncoupled density functional theory level. The σ^{PV} of the heavy nuclei in hydrogen peroxide, disulfane and diselane (H_2X_2 with $X=^{17}O$, ^{33}S, ^{77}Se) computed at the coupled cluster singles and doubles level are found to typically deviate from their electron-uncorrelated counterparts by approximately 20%, while in 2-fluorooxirane, electron correlation alters σ^{PV} of individual nuclei by almost a factor of 2. It is therefore imperative in the accurate prediction of parity-nonconserving phenomena in NMR experiments that systematically improvable electron-correlating electroweak quantum chemical approaches, such as those presented in this study, are employed.

DOI: 10.1103/PhysRevA.74.032105 PACS number(s): 31.15.Ew, 31.30.Jv, 11.30.Er, 12.15.Ji

I. INTRODUCTION

50 years after Lee and Yang's [1] Nobel-prize-winning suggestion to experimentally challenge the conservation of parity in processes involving the weak force, parity violation is nowadays a well established phenomenon in particle, nuclear and atomic physics but remains undetected in molecular physics despite numerous, unsuccessful attempts (see, for example, the recent review [2]). In 1966 Yamagata [3] pointed out that the parity-violating weak force induces an energy difference between enantiomers, the nonidentical mirror images of a chiral (handed) molecule. Approximately a decade later, Letokhov [4] emphasized that parity-violating interactions should additionally lead to resonance frequency differences in the electronic, vibrational, and rotational spectra of enantiomers. The order of magnitude of such line splittings, including those to be expected for nuclear-magnetic-resonance-(NMR)-shielding constants, were subsequently estimated by Gorshkov, Kozlov, and Labzowsky [5].

Barra, Robert, and Wiesenfeld [6,7] discussed in detail the possibility and experimental requirements of detecting molecular parity violation as line splittings between the NMR spectra of enantiomers and reported the first quantitative numerical calculations of differences in the NMR-shielding constants, performed in the framework of a semiempirical relativistically parameterized extended Hückel theory. Line splittings computed for fixed chiral conformations of some thallium, platinum, and lead containing compounds were on the order of a few millihertz, and thus considered to be only slightly below the resolution limit in NMR spectroscopy at that time [6]. Since then, NMR spectroscopy is considered to be one of the most promising techniques for a successful measurement of molecular parity violation.

Before parity-violating NMR line splittings can be detected, two chief obstacles have to be overcome, namely, (1) molecular compounds have to be synthesized for which large parity-violating NMR effects can be expected and (2) accurate and reliable predictions of parity-violating NMR line splittings are required to identify said compounds and interpret experimental results.

A semiempirical computational approach [6,7] is not ideally suited to provide quantitatively accurate and reliable predictions, and we therefore have presented previously [8] an *ab initio* approach to parity-violating NMR-shielding constants in chiral molecules within the framework of electroweak quantum chemistry reflecting the unification of electromagnetic and weak interactions within electroweak theory. Our initial *ab initio* approach towards parity-violating NMR effects utilized the random phase approximation (RPA), therefore neglecting electron correlation, as did a slightly later study by Soncini, Faglioni, and Lazzeretti [9] which was performed within the same framework. Recently, Weijo, Manninen, and Vaara [10] reported parity-violating NMR-shielding and indirect spin-spin coupling constants in CHBrClF and CHBrFI calculated within the random phase approximation and density functional theory (DFT). Compared to RPA level computations, deviations up to a factor of 2 were obtained for the shielding constants of individual nuclei in these systems when DFT was utilized. We anticipated [8] however, based on our previous investigations on parity-violating potentials [11], that the impact of electron correlation on the parity-violating NMR-shielding constants in hydrogen peroxide is much smaller, on the order of about 20%.

These findings have motivated us to report herein our detailed study on the effect of electron correlation for parity-violating NMR-shielding constants in hydrogen peroxide,

*Electronic address: R.Berger@fias.uni-frankfurt.de

disulfane, diselane and 2-fluorooxirane. 2-fluorooxirane is a chiral molecule with a high barrier for stereomutation. It is composed exclusively of light elements that possess, apart from oxygen, naturally occurring isotopes with a nuclear spin quantum number $I=1/2$. Nuclei with $I=1/2$ are particularly favorable for NMR experiments targeted towards a measurement of parity-violating effects. The other studied molecules, namely the dihydrogen dichalcogenides (H_2X_2), serve essentially as benchmark systems. Only in diselane does a naturally occurring isotope with $I=1/2$ exist for the heavy nucleus, and thus chiral diselane derivatives with sufficiently high barrier for stereomutation may in principle also be of experimental interest.

Herein we report the parity-violating NMR-shielding constants computed at an *ab initio* level within the framework of a multiconfiguration linear response and coupled-cluster linear response approach to electroweak quantum chemistry. These methods represent a sound starting point for the systematic investigation of molecular parity-violating effects, crucial for the preparation and interpretation of experiments aiming at the first detection of parity-violating effects in chiral molecular systems. For comparison we present results obtained at the economically favorable, but currently not systematically improvable, DFT level, which in principle allows treatment of chiral molecular systems with a large number of nuclei.

II. METHODOLOGY

The weak interaction is mediated by the charged $W^{\pm}$ bosons and the neutral Z^0 boson. The latter boson is expected to be responsible for the dominant parity-violating contributions in molecules composed of electrons and stable nuclei. In the low energy regime, exchange of virtual Z^0 bosons results in neutral current interactions between two quarks, between two leptons or between a quark and a lepton. In molecular systems with stable nuclei a leading parity-violating contribution should arise from the electron-nucleus (electron-quark) neutral current interactions. A further source for molecular parity nonconservation are parity-violating interactions within the nucleus (parity-violating meson-nucleon interactions) that induce a nuclear anapole moment [12] to which the electrons can couple electromagnetically.

The effective Hamiltonian for the parity-violating term of the electron-nucleus neutral current interaction in a molecular system with n electrons and N nuclei reads in the non-relativistic limit (see, for instance, Refs. [2,6,8,11,13]):

$$\begin{aligned}\hat{H}_{\mathrm{PV}}^{(e\text{-nucl})} &= \hat{H}_{\mathrm{PV}}^{(e\text{-nucl},1)} + \hat{H}_{\mathrm{PV}}^{(e\text{-nucl},2)} + \hat{H}_{\mathrm{PV}}^{(e\text{-nucl},3)} \\ &= \sum_{i=1}^{n} [\hat{h}_{\mathrm{PV}}^{(1)}(i) + \hat{h}_{\mathrm{PV}}^{(2)}(i) + \hat{h}_{\mathrm{PV}}^{(3)}(i)] \\ &= \frac{G_{\mathrm{F}}}{2\sqrt{2}m_e c} \sum_{i=1}^{n} [\sum_{A=1}^{N} Q_{\mathrm{W}}(A)\{\hat{\vec{p}}_i \cdot \hat{\vec{s}}_i, \delta(\vec{r}_i - \vec{r}_A)\} \\ &\quad + \sum_{A=1}^{N} (-\lambda_A)(1 - 4\sin^2\theta_{\mathrm{W}})\Big\{\hat{\vec{p}}_i \cdot \hat{\vec{I}}_A, \delta(\vec{r}_i - \vec{r}_A)\Big\} \\ &\quad + \sum_{A=1}^{N} 2i\lambda_A(1 - 4\sin^2\theta_{\mathrm{W}})(\hat{\vec{s}}_i \times \hat{\vec{I}}_A) \cdot [\hat{\vec{p}}_i, \delta(\vec{r}_i - \vec{r}_A)]], \end{aligned} \tag{1}$$

with G_{F} representing the Fermi constant, m_e the electron rest mass, c the speed of light in vacuum, $Q_{\mathrm{W}}(A)$ the electroweak charge with $Q_{\mathrm{W}}(A)=Z_A(1-4\sin^2\theta_{\mathrm{W}})-N_A$, Z_A the number of protons in nucleus A, N_A its number of neutrons, $\hat{\vec{I}}_A$ the dimensionless reduced nuclear spin operator of nucleus A, θ_{W} the Weinberg angle, $\hat{\vec{p}}_i$ the linear momentum operator of electron i and $\hat{\vec{s}}_i$ its dimensionless reduced spin operator, $\delta(\vec{x})$ the Dirac delta distribution, $\vec{r}_\mu$ the position vector of particle μ, $[\cdot,\cdot]$ the commutator and $\{\cdot,\cdot\}$ the anticommutator. The coefficient λ_A is a nuclear state-dependent factor on the order of unity [7,14–17]. A pointlike nucleus has been assumed in the derivation of the effective Hamiltonian. Finite nuclear sizes can be included by replacing the Dirac delta distribution $\delta(\vec{r}_i-\vec{r}_A)$ by an appropriate nucleon density distribution $\rho_A(\vec{r})$. While $\hat{h}_{\mathrm{PV}}^{(1)}(i)$ is nuclear spin-independent, the operators $\hat{h}_{\mathrm{PV}}^{(2)}(i)$ and $\hat{h}_{\mathrm{PV}}^{(3)}(i)$ depend on the nuclear spin $\vec{I}_A$ and therefore are particularly important for parity-violating effects in NMR spectra of chiral compounds [6,7,13]. Parity-violating contributions to the NMR-shielding constants caused by neutral current interactions between two electrons are expected to play only a minor role and are thus neglected in the present work.

The effective Hamiltonian for the electromagnetic interaction between electrons and the nuclear anapole moment is given by

$$\begin{aligned}\hat{H}_{\mathrm{PV}}^{(e\text{-nucl,anapole})} = \sum_{i=1}^{n} \Bigg[&\sum_{A=1}^{N} (-\beta_A)\{\hat{\vec{p}}_i \cdot \hat{\vec{I}}_A, \delta(\vec{r}_i - \vec{r}_A)\} \\ &+ \sum_{A=1}^{N} 2i\beta_A(\hat{\vec{s}}_i \times \hat{\vec{I}}_A) \cdot [\hat{\vec{p}}_i, \delta(\vec{r}_i - \vec{r}_A)]\Bigg]. \end{aligned} \tag{2}$$

Here β_A represents a nuclear state-dependent parameter. The operator $\hat{H}_{\mathrm{PV}}^{(e\text{-nucl,anapole})}$ has precisely the same structure as $\hat{H}_{\mathrm{PV}}^{(e\text{-nucl},2)}+\hat{H}_{\mathrm{PV}}^{(e\text{-nucl},3)}$ and can therefore be included on the same footing as the corresponding neutral current interaction [13,15,18]. Thus we use in the evaluation of the matrix elements of $\hat{H}_{\mathrm{PV}}^{(e\text{-nucl},2)}$ and $\hat{H}_{\mathrm{PV}}^{(e\text{-nucl},3)}$ the coefficient $\lambda_A=-1$ for all nuclei [8]. Corresponding results can then be subsequently scaled with appropriate factors which account for the combined nuclear anapole and weak current contribution.

In the presence of magnetic fields, the linear momentum operator is altered according to the minimal coupling prescription. An external homogeneous magnetic field will give rise to additional terms in the parity-violating Hamiltonian, leading to a diamagnetic contribution in the parity-violating NMR-shielding tensor. This contribution vanishes, however, if the gauge origin is chosen to be identical with the position of the nucleus of interest [13], as was done in the present work. Furthermore, the diamagnetic term is an antisymmetric tensor [9] leaving the isotropic parity-violating NMR-shielding constant unaffected.

The leading contribution to the parity-violating NMR-shielding tensor $\boldsymbol{\sigma}^{\mathrm{PV}}(A)$ for nucleus A, with components $\sigma_{kl}^{\mathrm{PV}}(A)$ $(k,l=x,y,z)$ (see also Refs. [5,6,8–10,13]) arises in linear response theory as

$$\sigma_{kl}^{\mathrm{PV}}(A) = \frac{e\hbar}{2m_e}\frac{G_{\mathrm{F}}}{2\sqrt{2}m_e c}(-\lambda_A)(1-4\sin^2\theta_{\mathrm{W}}) \times \langle\langle \hat{P}_k^{\mathrm{PV},(2)}(A); \hat{P}_l^{\mathrm{orb}}\rangle\rangle_{\omega_1=0} (\gamma_A \hbar)^{-1}, \quad (3)$$

where $\langle\langle \cdot;\cdot\rangle\rangle_{\omega_1}$ is the linear response function (see also Ref. [11]) and γ_A the magnetogyric ratio of nucleus A. The operator $\hat{\hat{P}}^{\mathrm{PV},(2)}(A)$ is defined by

$$\hat{\hat{P}}^{\mathrm{PV},(2)}(A) = \sum_{i=1}^{n} \{\hat{\vec{p}}_i, \delta(\vec{r}_i - \vec{r}_A)\}, \quad (4)$$

while $\hat{\hat{P}}^{\mathrm{orb}}$, which arises due to the orbital Zeeman term, is given by

$$\hat{\hat{P}}^{\mathrm{orb}} = \sum_{i=1}^{n} \hat{\hat{l}}_{i,\mathrm{O}}, \quad (5)$$

with $\hat{\hat{l}}_{i,\mathrm{O}}$ denoting the orbital angular momentum of electron i with respect to the gauge origin.

Higher order contributions to $\boldsymbol{\sigma}^{\mathrm{PV}}(A)$ (to order $G_{\mathrm{F}}c^{-3}$) stem, for instance, from $\hat{H}_{\mathrm{PV}}^{(e\text{-nucl},1)}$ in combination with the magnetic hyperfine interaction term or from $\hat{H}_{\mathrm{PV}}^{(e\text{-nucl},3)}$ together with the orbital Zeeman and the spin-orbit coupling term (see Ref. [5]). Some further terms on the same order arising in the Breit-Pauli framework have recently been identified by Weijo, Manninen, and Vaara [10]. In our present work, which focuses mainly on molecules containing light nuclei, we restrict ourselves to the leading contribution to the parity-violating NMR-shielding constant as given in Eq. (3).

III. COMPUTATIONAL DETAILS

For hydrogen peroxide and its heavier homologues we employ the same geometries as utilized in previous studies [8,19–21]. The C_2 point group symmetry is maintained throughout and, except for the dihedral angle α, all other internal structural parameters are held constant. The frozen nuclear distances r and bond angles β are $r_{\mathrm{OO}}=149.0$ pm, $r_{\mathrm{OH}}=97.0$ pm, $\beta_{\mathrm{OOH}}=100°$, $r_{\mathrm{SS}}=205.5$ pm, $r_{\mathrm{SH}}=135.2$ pm, $\beta_{\mathrm{SSH}}=92°$, $r_{\mathrm{SeSe}}=248.0$ pm, $r_{\mathrm{SeH}}=145.0$ pm, and $\beta_{\mathrm{SeSeH}}=92°$. For 2-fluorooxirane we use the equilibrium structure employed in previous studies [8,22]. Corresponding Cartesian coordinates are reported in the EPAPS material [23].

The family of correlation-consistent polarized valence multiple zeta basis sets (cc-pV*N*Z with N=D,T,Q,5,6) is used [24–28], which is referred to as aug-cc-pV*N*Z when the set is augmented by additional diffuse functions [24,25,29]. The cc-pV*N*Z basis sets are also used in uncontracted form with additional tight s and p functions (henceforth referred to as cc-upV*N*Z+*m*s*n*p). Exponents α_i for the m additional s- and n additional p-Gaussian primitives are generated as an even tempered series $\alpha_i=\alpha_{\mathrm{max,orig}}\beta^i$, $i=1,2,\ldots,m$ or n, with $\alpha_{\mathrm{max,orig}}$ being the largest exponent of the s- or p-primitive functions, respectively, of the original cc-pV*N*Z basis set. Here β is chosen to be 8.0. These large uncontracted basis sets are only used for the nonhydrogen atoms, whereas the basis set for hydrogen is in these cases restricted to the uncontracted cc-pVDZ set.

In addition to the correlation consistent basis sets we also employ large even-tempered basis sets to approach the RPA limit of the parity-violating NMR-shielding constants for the ^{17}O nucleus in hydrogen peroxide at 45° dihedral angle. These basis sets are generated according to $\alpha_i^{\mathrm{orb}}=\gamma\beta^{N-i}$ with $i=1,2,\ldots,N$ and $N=26$. The values $\alpha_{26}^{\mathrm{orb}}=\gamma=(2/100)a_0^{-2}$ and $\alpha_1^{\mathrm{orb}}=500\,000\,000\ a_0^{-2}$ are chosen as the smallest and largest exponent of this list, respectively. The notation s:1⋯25 implies that exponents from this list ranging from $i=1$ to $i=25$ are employed for the s-primitive Gaussian functions. A similar notation is used for p, d, and f functions. Even-tempered basis sets for sulfur and selenium are generated from the same list used for oxygen.

For 2-fluorooxirane we also employ the triple zeta basis set with two sets of polarization functions (TZ2P) [30] which we used in Refs. [8,22]. This TZ2P basis set was reported in Ref. [30] (see also Ref. [31]) and comprises for nonhydrogen atoms Dunning's [5s4p] contraction [32] of Huzinaga's (10s6p) set of primitive Gaussians [33] augmented by two sets of polarizing d functions (exponents: $1.2a_0^{-2}$ and $0.4a_0^{-2}$ on carbon, $1.35a_0^{-2}$ and $0.45a_0^{-2}$ on oxygen, and $2.0a_0^{-2}$ and $0.6667a_0^{-2}$ on fluorine) and for hydrogen Dunning's [3*s*] contraction [32] of Huzinaga's (5s) set of primitive Gaussians with exponents scaled by 25/16 (to fit a Slater orbital with exponent $\zeta=1.25a_0^{-1}$) augmented by two sets of polarizing p functions (exponents: $1.5a_0^{-2}$ and $0.5a_0^{-2}$). Details of the basis set are reported in [23].

All calculations are performed with spherical Gaussians (including those with the TZ2P basis set). The common gauge origin is placed at the nucleus of interest and, thus, gauge including atomic orbitals (GIAOs) [34] are not used in the present study. We employ a numerical value of Fermi's constant $G_{\mathrm{F}}=2.22254\times10^{-14}E_{\mathrm{h}}a_0^3$ and a Weinberg angle corresponding to $\sin^2\theta_{\mathrm{W}}=0.2319$. In the present work only the isotropic contribution $\sigma^{\mathrm{PV}}=(\sigma_{xx}^{\mathrm{PV}}+\sigma_{yy}^{\mathrm{PV}}+\sigma_{zz}^{\mathrm{PV}})/3$ of the tensor $\boldsymbol{\sigma}^{\mathrm{PV}}$ is reported as the parity-violating NMR-shielding constant.

We utilize the linear response treatment in the complete active space self-consistent field (CASSCF) approach as described in Refs. [35,36] and the coupled cluster (CC) linear response approach described in Refs. [37,38]. All electrons are correlated in the CC linear response calculations, whereas the active spaces selected for the CASSCF approach comprises only the valence orbitals (full valence) for disulfane and additionally also the oxygen 1s orbitals for hydrogen peroxide (full valence +1s). In the density functional theory (DFT) framework we employ exchange-correlation density-only functionals (i.e., exchange-correlation functionals independent of the current density). This permits an uncoupled DFT treatment in which the corresponding linear response equations reduce to simple sum-over-states expressions, with states described by single replacement Slater de-

terminants and energy denominators given as orbital energy differences. All calculations are performed with modified versions [8] of DALTON 1.2.1 [39] (RPA, CASSCF, CC) and DALTON 2.0 [40] (DFT, CC).

IV. RESULTS AND DISCUSSION

Parity-violating NMR-shielding constants for the ^{17}O nucleus in hydrogen peroxide at different dihedral angles, computed with various basis sets and methods, are reported in Table I. Furthermore, σ^{PV} (^{17}O) is plotted as a function of the dihedral angle in Fig. 1 for various methods and the upVQZ+4s7p basis set on oxygen. A negative (or positive) value of $\sigma^{PV}(X)$ indicates that the NMR-shielding constant of hydrogen peroxide in the *P* conformation is, for the present choice of λ_A, lowered (or raised) due to the parity-violating forces. The parity-violating NMR-shielding constant of the mirror-image *M* conformation has precisely the same magnitude but opposite sign. Overall a $-\sin(2\alpha)$-like dependence of σ^{PV} on the dihedral angle α is observed for all basis sets and methods employed herein. Neglecting the sign, we observe that this dependence parallels the behavior of the parity-violating potential (see, e.g., Refs. [11,19–21,41–45]) and several other pseudoscalar properties such as the optical rotation in hydrogen peroxide. At the dihedral angles $\alpha=0°$ and $\alpha=180°$ the parity-violating NMR-shielding constant vanishes due to symmetry. A similar dihedral angle dependent behavior of the heavy nucleus NMR-shielding constant is also observed for disulfane and diselane (see Table II). Because σ^{PV}(X) in H_2X_2 is close to zero for dihedral angles around 90°, we will not take these values into account below, when general trends for the various methods and basis sets are discussed.

Table III illustrates the basis set dependence of $\sigma^{PV}(^{17}O)$ in hydrogen peroxide at the RPA level. Previously, in Ref. [8], we reported results for the standard aug-cc-pV*N*Z basis. To speed up convergence of the parity-violating NMR-shielding constants with increasing cardinal number *N*, the still contracted aug-cc-pV*N*Z basis set was augmented in Ref. [8] by several uncontracted steep p functions (basis set denoted as aug-cc-pV*N*Z+p in Table III). In the present study we initially start with the uncontracted cc-pV*N*Z basis sets and subsequently augment them by several tight s and p functions while still maintaining a small basis set on hydrogen (see computational details above). This series of basis sets yields already at the level of upVTZ+3p quite satisfactory results. Increase of the cardinal number *N* changes $\sigma^{PV}(^{17}O)$ by less than 3%, and additional s and p functions give rise to further changes of about 3%. Calculations with larger uncontracted even-tempered sets show that the results depend only moderately on the quality of the hydrogen basis set. We observe changes of less than 1% when using an uncontracted aug-cc-pVDZ set instead of an uncontracted cc-pVDZ set on hydrogen. Even a large even-tempered sp substratum does not induce substantial changes and further polarization with additional d functions alters results at the 0.1% level. While tight d functions on oxygen are apparently of minor importance, further polarization with additional f functions leads to more pronounced changes on the order of 2%. The parity-violating NMR-shielding constant of -60.9×10^{-10} ppm obtained with the O(s:1···25,p:2···26,d:2···26,f:2···23,g:20···23)/H(s:1···25,p:2···24) basis set [$\sigma^{PV}(^{17}O)=-61.0\times10^{-10}$ ppm if the common gauge origin is shifted to the other oxygen nucleus] should be close to the RPA limit, which we may estimate to be $(-61\pm3)\times10^{-10}$ ppm, within the current framework.

Table I shows that electron correlation has a considerable effect on the parity-violating NMR-shielding constants in hydrogen peroxide. Both coupled cluster singles and doubles (CCSD) and CASSCF predict parity-violating NMR-shielding constants being larger (more positive) than at the RPA level for all dihedral angles, whereas DFT with the gradient corrected BLYP functional [46,47] predicts the absolute value of $\sigma^{PV}(^{17}O)$ to be always larger than the corresponding value at the RPA level. The second-order approximate coupled cluster singles and doubles model CC2 gives results quite similar to CCSD, and is computationally cheaper than CCSD, however, these results are systematically (marginally) smaller. Deviations between CC2 and CCSD are around 2% for dihedral angles below 90° and about 6% for larger angles. Inclusion of electron correlation at the CASSCF level (full valence +1s) leads to smaller corrections (up to 10% compared to RPA) to $\sigma^{PV}(^{17}O)$ than predicted at the CCSD level (changes up to about 25% compared to RPA). Typically CASSCF results are halfway between RPA and CCSD, with correlation corrections being larger for the uncontracted basis sets when the dihedral angles are smaller than 90°. As expected, convergence of $\sigma^{PV}(^{17}O)$ with increasingly larger basis sets is slower for CC and CASSCF methods than for HF, and at the CCSD level is still not reached for the upV5Z+3p basis, especially at large dihedral angles. CASSCF (full valence +1s) results appear to be almost converged for this basis set. Presently we can not ascertain whether CASSCF (full valence+1s) or CCSD results are more accurate. At small dihedral angles the deviations are more pronounced, whereas close to the equilibrium structure ($\alpha\approx110°$) CASSCF and CCSD do not deviate too strongly. Judging on the basis of the BLYP data, DFT, while being computationally very economical, does not appear to provide reliable results for correlation corrections to $\sigma^{PV}(^{17}O)$. While different functionals may give more promising results, at present there appears to be no systematic improvement when compared to RPA. We note in passing that DFT seems to perform reasonably well for parity-violating potentials (V_{PV}) in hydrogen peroxide [20,48], but it has been observed for CHBrClF that this method can also give rise to widely varying V_{PV} values [49]. To provide an estimate of the full configuration interaction results for $\sigma^{PV}(^{17}O)$, it is therefore imperative to go beyond the CCSD level and include triples corrections, preferably iteratively rather than perturbatively.

For the heavier homologues of hydrogen peroxide the inclusion of electron correlation indicates a different trend. Here both CC2 and CCSD predict parity-violating NMR-shielding constants of the heavy nuclei always smaller in magnitude than those computed at the RPA level, whereas DFT with the BLYP functional predicts that the absolute value of σ^{PV} for the heavy nuclei is always larger than the

TABLE I. Isotropic parity-violating NMR-shielding constant σ^{PV} given in 10^{-10} ppm for the oxygen nuclei ^{17}O in the *P*-enantiomer of H_2O_2 as computed for various dihedral angles α within the random phase approximation (RPA), the uncoupled density functional theory framework using the BLYP functional, the complete active space self-consistent field (CASSCF) method, and the coupled cluster linear response approach using the CC2 and the CCSD methods. Several samples from the family of the correlation-consistent polarized valence multiple zeta basis sets (cc-pV*N*Z with *N*=D, T, Q, 5, 6) augmented by additional diffuse functions (aug-cc-pV*N*Z) and, in uncontracted form, augmented with additional tight s and p functions (cc-upV*N*Z+*m*s*n*p) are employed. In addition, an even-tempered basis set is used on oxygen (see text for details).

Method	Basis set	α=30°	α=45°	α=60°	α=90°	α=120°	α=150°
RPA	aug-cc-pVDZ[a]	−34.94	−39.79	−34.14	−0.9217	31.61	31.97
	aug cc-pVTZ[a]	−40.23	−46.00	−39.69	−1.514	36.98	38.43
	aug-cc-pVQZ[a]	−44.36	−50.67	−43.62	−1.276	40.86	41.83
	aug-cc-pV5Z[a]	−48.46	−55.36	−47.70	−1.516	44.51	45.63
	O(25s25p5d)[b]/H(aug-upVDZ)	−54.63	−62.48	−53.80	−1.664	50.23	51.63
	upVDZ+3p	−47.95	−53.72	−44.45	4.672	52.33	51.92
	upVTZ+3p	−53.85	−60.80	−51.85	−1.899	48.03	50.10
	upVQZ+3p	−53.64	−60.83	−52.38	−3.660	45.47	48.01
	upV5Z+3p	−52.43	−59.76	−51.73	−4.032	44.40	47.20
	upV6Z+3p	−51.88	−59.20	−51.23	−3.352	45.40	48.01
	upVDZ+5s8p	−49.13	−55.05	−45.57	4.720	53.53	53.13
	upVTZ+5s8p	−54.82	−61.87	−52.76	−1.919	48.91	51.03
	upVQZ+4s7p	−54.31	−61.59	−53.05	−3.724	46.01	48.59
	upV5Z+4s7p	−52.83	−60.20	−52.10	−4.057	44.73	47.55
	upV6Z+3s6p	−51.95	−59.26	−51.28	−3.338	45.49	48.10
BLYP	aug-cc-pVDZ	−41.22	−45.04	−35.46	10.10	51.88	48.84
	aug-cc-pVTZ	−47.59	−52.18	−41.33	11.34	61.17	58.62
	aug-cc-pVQZ	−51.71	−56.84	−44.94	13.09	67.08	63.62
	aug-cc-pV5Z	−56.51	−62.05	−49.08	14.11	73.04	69.28
	O(25s25p5d)[b]/H(aug-upVDZ)	−64.22	−70.81	−56.21	15.76	82.95	78.87
	upVQZ+4s7p	−62.14	−67.56	−53.35	13.10	76.67	75.04
CASSCF	aug-cc-pVDZ	−33.13	−36.92	−30.45	3.067	34.77	33.89
	aug-cc-pVTZ	−39.35	−44.09	−36.69	2.637	40.68	40.72
	aug-cc-pVQZ	−43.32	−48.43	−40.12	3.496	45.05	44.33
	upVDZ+3p	−44.16	−48.10	−37.42	12.71	59.40	56.25
	upVTZ+3p	−49.78	−54.92	−44.74	5.365	53.40	52.97
	upVQZ+3p	−50.24	−55.73	−45.99	3.107	50.49	50.68
	upV5Z+3p	−49.81	−55.51	−46.09	2.337	49.31	49.88
	upVDZ+5s8p	−45.24	−49.29	−38.37	12.95	60.77	57.57
	upVTZ+5s8p	−50.68	−55.90	−45.53	5.471	54.38	53.94
	upVQZ+4s7p	−50.87	−56.43	−46.59	3.122	51.09	51.29
CC2	aug-cc-pVDZ	−29.96	−33.10	−26.60	5.829	36.01	34.17
	aug-cc-pVTZ	−35.06	−38.79	−31.26	6.792	43.26	41.89
	aug-cc-pVQZ	−38.25	−42.50	−34.36	7.377	46.88	44.97
	upVDZ+3p	−41.69	−45.16	−34.33	15.79	62.37	58.48
	upVTZ+3p	−47.39	−52.16	−42.19	6.679	53.93	53.59
	upVQZ+3p	−46.48	−51.48	−42.31	3.871	49.03	49.47
	upV5Z+3p	−44.45	−49.54	−40.98	3.282	47.14	48.10
	upVDZ+5s8p	−42.73	−46.30	−35.24	16.07	63.77	59.84
	upVTZ+5s8p	−48.23	−53.07	−42.90	6.824	54.93	54.58
	upVQZ+4s7p	−47.06	−52.14	−42.87	3.889	49.61	50.06
	upV5Z+4s7p	−44.79	−49.91	−41.28	3.306	47.50	48.45

TABLE I. (*Continued.*)

Method	Basis set	$\alpha=30°$	$\alpha=45°$	$\alpha=60°$	$\alpha=90°$	$\alpha=120°$	$\alpha=150°$
CCSD	aug-cc-pVDZ	−30.17	−33.21	−26.41	7.050	37.95	35.64
	aug-cc-pVTZ	−34.69	−38.31	−30.63	7.859	44.48	42.67
	aug-cc-pVQZ	−37.64	−41.67	−33.35	8.651	48.05	45.57
	upVDZ+3p	−41.40	−44.58	−33.32	17.98	65.36	60.76
	upVTZ+3p	−46.59	−51.08	−40.78	8.892	56.45	55.20
	upVQZ+3p	−45.60	−50.28	−40.77	6.278	51.65	51.04
	upV5Z+3p	−43.74	−48.49	−39.50	5.806	49.85	49.59
	upVDZ+5s8p	−42.43	−45.71	−34.20	18.33	66.85	62.17
	upVTZ+5s8p	−47.42	−51.97	−41.47	9.073	57.48	56.21
	upVQZ+4s7p	−46.16	−50.93	−41.30	6.330	52.27	51.65
	upV5Z+4s7p	−44.07	−48.85	−39.79	5.850	50.22	49.96

[a]Results from Ref. [8].
[b]O(s:1···25,p:2···26,d:20···24).

corresponding value at the RPA level. Full valence CASSCF values of $\sigma^{PV}(^{33}S)$ in disulfane are, for dihedral angles $\alpha < 90°$, again typically midway between the values obtained at the RPA and CCSD level. Similar to BLYP, however, the full valence CASSCF parity-violating NMR-shielding constants are, for dihedral angles $\alpha > 90°$, larger in magnitude than those obtained at the RPA level. Changes in the parity-violating NMR-shielding constant due to electron correlation are predicted at the CCSD level to be up to about 25%. Larger uncontracted basis sets typically lead to an increase of the absolute values of σ^{PV}, by a further 20% when explicitly calculated at the RPA level. These changes do not alter the overall scaling behavior with increasing charge of nucleus X in the series H_2X_2, X=O,S,Se, which we previously tentatively assumed to be approximately $Z^{3\pm1}$ when the NMR-shielding constants in parts per million are translated to NMR resonance frequency differences.

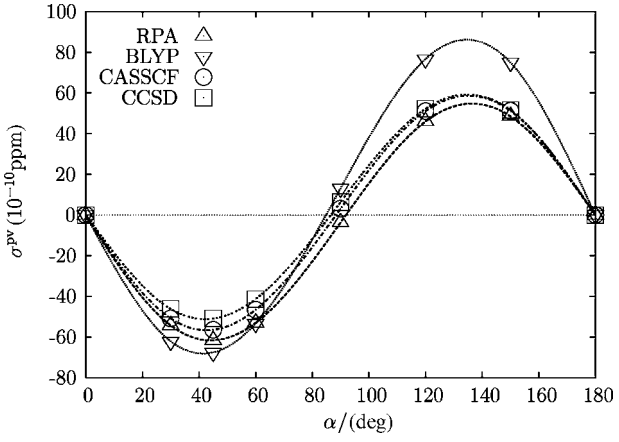

FIG. 1. Dihedral angle (α) dependence of the isotropic parity-violating NMR-shielding constant σ^{PV} for the oxygen nuclei ^{17}O in the P enantiomer of H_2O_2 as computed with the upVQZ+4s7p basis set within the random phase approximation (RPA), the complete active space self-consistent field (CASSCF) linear response approach, the coupled cluster linear response approach using the CCSD method and the uncoupled density functional theory framework using the BLYP functional (see text for details of methods and basis set).

In 2-fluorooxirane correlation effects for the heavy $I=1/2$ nuclei are much more pronounced (up to about 70%), while for ^{17}O electron correlation effects are quite small (below 3%), at least for the relatively small contracted basis sets employed in the present study. Most importantly, at the CCSD level the difference between absolute values of the parity-violating NMR-shielding constants of the $^{13}C^2$ and $^{13}C^3$ nucleus is further increased with the latter constant being more than three times larger than the former despite C^2 being the stereogenic centre of the molecule. This is attributed to a smaller electron density at C^2 caused by the strongly electronegative fluorine atom. Extended basis sets will be required to achieve convergence of the parity-violating NMR-shielding constants for 2-fluorooxirane, particularly at the correlated level. This is, however, beyond the scope of our present study.

V. CONCLUSION AND OUTLOOK

In this study, we provided benchmark results on the parity-violating NMR-shielding constants in hydrogen peroxide and investigated the heavier disulfane and diselane homologues as well as the "ordinary" chiral compound 2-fluorooxirane. Although such simplified rules of thumb have to be viewed with considerable caution, parity-violating NMR-frequency splittings between enantiomers, as computed in the present work, scale approximately with the second to fourth order of the nuclear charges for the heavy centers in the H_2X_2 series.

Hence, one arrives at the same conclusions regarding the general prospects of NMR measurments of parity-violating effects in chiral molecules as discussed previously [8]. Correlation corrections in hydrogen peroxide are significant but do not exceed about 15% at the CASSCF level (with all valence orbitals and the 1s orbitals on oxygen included in the active space) and about 25% on the CC2 and CCSD level, maintaining a consistent sign for these corrections. BLYP appears to be unreliable in this respect and preliminary re-

TABLE II. Isotropic parity-violating NMR-shielding constant σ^{PV} given in 10^{-10} ppm for the ^{33}S and ^{77}Se nuclei in the *P* enantiomer of H_2S_2 and H_2Se_2, respectively, at various dihedral angles α (see text and caption of Table I for details). Furthermore, isotropic parity-violating NMR-shielding constants (in 10^{-10} ppm) are given for the ^{13}C, ^{17}O, and ^{19}F nuclei in (*R*)-2-fluorooxirane computed in the RPA and with the CC2 and CCSD linear response approach with the aug-cc-pVTZ basis set and a triple zeta basis set with two polarization functions (TZ2P).

	Method	Basis set	$\alpha=30°$	$\alpha=45°$	$\alpha=60°$	$\alpha=90°$	$\alpha=120°$	$\alpha=150°$
(*P*)-$H_2{}^{33}S_2$	RPA	aug-cc-pVDZ[a]	597.7	710.0	669.9	269.8	−187.8	−274.0
		aug-cc-pVTZ[a]	684.3	803.6	750.4	281.2	−242.4	−342.8
		aug-cc-pVQZ[a]	693.9	821.5	774.2	299.4	−243.5	−350.2
		aug-cc-pV5Z[a]	778.0	920.5	866.8	333.9	−274.3	−396.1
	S(25s25p5d)[b]/H(aug-upVDZ)		820.2	970.1	914.2	362.4	−262.4	−389.2
	BLYP	aug-cc-pVDZ	734.1	856.4	793.7	298.0	−249.3	−348.5
		aug-cc-pVTZ	839.6	966.0	882.7	302.3	−315.7	−428.2
		aug-cc-pVQZ	848.2	985.0	908.6	322.1	−313.7	−431.5
	CASSCF	aug-cc-pVDZ	597.3	698.5	647.7	237.3	−224.8	−305.0
		aug-cc-pVTZ	682.0	788.2	722.6	244.1	−281.0	−374.5
	CC2	aug-cc-pVDZ	527.8	622.8	584.9	239.9	−146.3	−222.0
		aug-cc-pVTZ	599.5	697.8	645.6	240.1	−198.2	−283.3
		aug-cc-pVQZ	602.5	707.5	661.7	257.3	−189.7	−280.7
	CCSD	aug-cc-pVDZ	554.9	656.0	616.9	250.8	−163.1	−244.5
		aug-cc-pVTZ	617.1	720.3	668.9	252.0	−202.9	−292.4
		aug-cc-pVQZ	619.0	728.8	684.3	270.6	−192.4	−288.3
(*P*)-$H_2{}^{77}Se_2$	RPA	aug cc-pVDZ[a]	1403	1652	1531	490.8	−668.4	−887.5
		aug-cc-pVTZ[a]	1521	1797	1668	507.5	−783.3	−993.8
		aug-cc-pVQZ[a]	1587	1866	1721	520.2	−808.7	−1024
	Se(25s25p11d)[c]/H(aug-upVDZ)		1735	2037	1879	574.9	−866.5	−1109
	BLYP	aug-cc-pVDZ	1831	2105	1876	406.9	−1127	−1350
		aug-cc-pVTZ	2001	2311	2064	416.4	−1306	−1515
		aug-cc-pVQZ	2078	2387	2125	437.1	−1340	−1564
	CC2	aug-cc-pVDZ	1186	1385	1264	352.9	−619.4	−781.1
		aug-cc-pVTZ	1271	1488	1357	346.3	−727.4	−872.9
	CCSD	aug-cc-pVDZ	1235	1440	1314	362.1	−662.3	−830.8
		aug-cc-pVTZ	1290	1513	1385	363.3	−737.6	−891.9
			$^{13}C^2$	$^{13}C^3$	^{17}O	^{19}F		
(*R*)-C_2H_3FO	RPA	TZ2P[a]	−3.023	7.615	79.69	2.832		
		aug-cc-pVTZ[a]	−3.546	7.623	72.44	2.721		
	CC2	TZ2P	−1.299	9.553	88.82	5.987		
		aug-cc-pVTZ	−2.245	10.05	77.84	5.772		
	CCSD	TZ2P	−1.592	8.786	81.90	4.717		
		aug-cc-pVTZ	−2.400	9.053	72.73	4.468		

[a]Results from Ref. [8].
[b]S(s:1⋯25,p:2⋯26,d:20⋯24).
[c]Se(s:1⋯25,p:2⋯26,d:15⋯25).

sults with other popular density functionals give no clear indication of a systematic alleviation of this problem. While this does not exclude density functional theory *per se* for calculating parity-violating NMR-shielding constants, since the order of magnitude for the present case is correct, it does, however, raise some concerns about the reliability of correlation corrections computed on this level. Density functional results reported for parity-violating NMR-shielding constants of CHBrClF and CHBrFI in Ref. [10] can thus at present not be considered more accurate than the corresponding RPA results. For these compounds however, (further) relativistic effects will likely be of greater importance (see below). Our *ab initio* calculations of parity-violating NMR-shielding constants in 2-fluorooxirane, which contains light nuclei only,

TABLE III. Isotropic parity-violating NMR-shielding constant σ^{PV} given in 10^{-10} ppm computed within the RPA for the oxygen nuclei ^{17}O in the P enantiomer of H_2O_2 at a dihedral angle $\alpha=45°$ (see text and caption of Table I for details).

Basis set	RPA	Basis set	RPA
aug-cc-pVDZ[a]	−39.79	upVDZ+3p	−53.72
aug-cc-pVTZ[a]	−46.00	upVTZ+3p	−60.80
aug-cc-pVQZ[a]	−50.67	upVQZ+3p	−60.83
aug-cc-pV5Z[a]	−55.36	upV5Z+3p	−59.76
aug-cc-pV6Z	−57.89	upV6Z+3p	−59.20
aug-cc-pVDZ+p[a]	−58.85	upVDZ+5s8p	−55.05
aug-cc-pVTZ+p[a]	−58.85	upVTZ+5s8p	−61.87
aug-cc-pVQZ+p[a]	−59.65	upVQZ+4s7p	−61.59
aug-cc-pV5Z+p[a]	−60.13	upV5Z+4s7p	−60.20
		upV6Z+3s6p	−59.26
		aug-upVDZ+3p	−63.31
		aug-upVTZ+3p	−60.42
		aug-upVQZ+3p	−60.87
		aug-upV5Z+3p	−60.89
O(s:1⋯25,p:2⋯26,d:20⋯24)/H(upVDZ)			−62.94
O(s:1⋯25,p:2⋯26,d:20⋯24)/H(aug-upVDZ)			−62.48
O(s:1⋯25,p:2⋯26,d:2⋯26)-/H(aug-upVDZ)			−62.38
O(s:1⋯25,p:1⋯26,d:1⋯26,f:20⋯23)/H(upVDZ)			−61.78
O(s:1⋯25,p:1⋯26,d:1⋯26,f:20⋯23)/H(s:1⋯25,p:1⋯24)			−61.00
O(s:1⋯25,p:2⋯26,d:2⋯26,f:20⋯23)/H(aug-upVDZ)			−60.95
O(s:1⋯25,p:2⋯26,d:2⋯26,f:20⋯23)/H(s:1⋯25,p:20⋯23)			−60.89
O(s:1⋯25,p:2⋯26,d:2⋯26,f:20⋯23)/H(s:1⋯25,p:2⋯24)			−60.77
O(s:1⋯25,p:2⋯26,d:2⋯26,f:20⋯23)/H(s:1⋯25,p:2⋯24,d:20⋯23)			−60.77
O(s:1⋯25,p:2⋯26,d:2⋯26,f:2⋯23)/H(s:1⋯25,p:2⋯24)			−60.77
O(s:1⋯25,p:2⋯26,d:2⋯26,f:2⋯23,g:20⋯23)/H(s:1⋯25,p:2⋯24)			−60.85

[a]Results from Ref. [8].

demonstrate that electron correlation contributions might indeed alter σ^{PV} of individual nuclei by about a factor of two and are therefore imperative when predicting parity-nonconserving effects in the NMR spectra of chiral molecules accurately. Changes of this size have been observed in Ref. [10] for CHBrClF and CHBrFI when RPA and uncoupled DFT results were compared.

Even with extended atomic basis sets, convergence of parity-violating NMR-shielding tensors is notoriously difficult to achieve. This is, to some extent, due to the use of a common gauge origin in our procedure, instead of either employing gauge including atomic orbitals [34] or using an individual gauge for localized orbitals [50]. Nevertheless, large basis sets are still required in these cases, particularly if Gaussian basis set expansions are involved, because the operator $\hat{P}^{PV,(2)}(A)$ couples atomic s and p functions and requires an accurate description of both the electronic wavefunction and its first derivative near the nuclei of interest.

Our results reported here for σ^{PV} include one electron terms to first order in Fermi's constant and to order c^{-1}. Further relativistic corrections are expected to remain small in hydrogen peroxide and are perhaps less important than the triples contribution to σ^{PV} within a CCSDT or CCSD(T) treatment. An approximate relativistic enhancement factor (see also Ref. [6]), which shall correct the behavior of the electronic wave function near the nuclei, is about 1.03 for ^{17}O using the equation given in Ref. [15]. This may provide a first estimate for the order of magnitude for one of the various corrections in hydrogen peroxide.

In heavier systems, these additional relativistic effects become sizeable and require (relativistic) four-component schemes [51] or (quasirelativistic) two-component approaches for quantitatively accurate theoretical predictions. Our group is actively pursuing this research direction using the latter approach [52].

ACKNOWLEDGMENTS

We thank Jason Stuber and Sophie Nahrwold for stimulating discussions as well as Trond Saue and Peter

Schwerdtfeger for providing us with a copy of their manuscript [51] that we recently received. We are indebted to the Volkswagen Foundation, to the Fonds der Chemischen Industrie, to the Deutsche Forschungsgemeinschaft, and to the Graduiertenkolleg 352 for financial support. The Norddeutscher Verbund für Hoch- und Höchstleistungsrechnen (HLRN) and the Center for Scientific Computing (CSC) Frankfurt is acknowledged for providing computer time.

[1] T. D. Lee and C. N. Yang, Phys. Rev. **104**, 254 (1956).
[2] R. Berger, in *Relativistic Electronic Structure Theory, Part: 2, Applications*, edited by P. Schwerdtfeger (Elsevier, Amsterdam, 2004), pp. 188–288.
[3] Y. Yamagata, J. Theor. Biol. **11**, 495 (1966).
[4] V. S. Letokhov, Phys. Lett.A **53**, 275 (1975).
[5] V. G. Gorshkov, M. G. Kozlov, and L. N. Labzowsky, Sov. Phys. JETP **55**, 1042 (1982).
[6] A. L. Barra, J. B. Robert, and L. Wiesenfeld, Phys. Lett. A **115**, 443 (1986).
[7] A. L. Barra, J. B. Robert, and L. Wiesenfeld, Europhys. Lett. **5**, 217 (1988).
[8] G. Laubender and R. Berger, ChemPhysChem **4**, 395 (2003). Note, that in this paper and the present work, $\lambda=-1$ has been used (instead of $\lambda=1$ as stated in this paper).
[9] A. Soncini, F. Faglioni, and P. Lazzeretti, Phys. Rev. A **68**, 033402 (2003).
[10] V. Weijo, P. Manninen, and J. Vaara, J. Chem. Phys. **123**, 054501 (2005).
[11] R. Berger and M. Quack, J. Chem. Phys. **112**, 3148 (2000).
[12] B. Ya. Zel'dovich, Sov. Phys. JETP **33**, 1531 (1957).
[13] A. L. Barra and J. B. Robert, Mol. Phys. **88**, 875 (1996).
[14] M. A. Bouchiat, in *New Trends in Atomic Physics*, edited by G. Grynberg and R. Stora (Les Houches, North-Holland, Amsterdam, 1984), Vol. 2, pp. 887–950.
[15] I. B. Khriplovich, *Parity Nonconservation in Atomic Phenomena* (Gordon and Breach Science, Philadelphia, 1991).
[16] Within the shell model of the nucleus and some further simplifying assumptions (see Refs. [15,18]) one obtains $\lambda_A=\pm\lambda(1/2-K)[2I(I+1)]^{-1}$ with $K=(I+1/2)(-1)^{I+1/2-l}$ and I being the nuclear spin quantum number, l being the orbital angular momentum of the valence nucleon, $\lambda=g_A/g_V\approx 1.25$ being the ratio of the weak axial vector and the weak vector coupling constants of the neutron beta decay (see [17]). The positive (negative) sign is selected, when a valence proton (neutron) carries the magnetic moment of the nucleus. For the proton, $\lambda_A=\lambda\approx 1.25$.
[17] K. Hagiwara *et al.*, Phys. Rev. D **66**, 010001 (2002).
[18] V. V. Flambaum and I. B. Khriplovich, Sov. Phys. JETP **52**, 835 (1980).
[19] J. K. Laerdahl and P. Schwerdtfeger, Phys. Rev. A **60**, 4439 (1999).
[20] R. Berger and C. van Wüllen, J. Chem. Phys. **122**, 134316 (2005).
[21] R. Berger, N. Langermann, and C. van Wüllen, Phys. Rev. A **71**, 042105 (2005).
[22] R. Berger, M. Quack, and J. Stohner, Angew. Chem., Int. Ed. **40**, 1667 (2001).
[23] See EPAPS Document No. E-PLRAAN-71-061607 for two additional tables with Cartesian coordinates of the 2-fluorooxirane structure and with contraction coefficients and exponents of the TZ2P basis set employed in this study. For more information on EPAPS, see http://www.aip.org/pubservs/epaps.html
[24] T. H. Dunning, Jr., J. Chem. Phys. **90**, 1007 (1989).
[25] D. E. Woon and T. H. Dunning, Jr., J. Chem. Phys. **98**, 1358 (1993).
[26] A. K. Wilson, D. E. Woon, K. A. Peterson, and T. H. Dunning, Jr., J. Chem. Phys. **110**, 7667 (1999).
[27] K. A. Peterson, D. E. Woon, and T. H. Dunning, Jr., J. Chem. Phys. **100**, 7410 (1994).
[28] A. K. Wilson, T. van Mourik, and T. H. Dunning, Jr., J. Mol. Struct. **388**, 339 (1996).
[29] R. A. Kendall, T. H. Dunning, Jr., and R. J. Harrison, J. Chem. Phys. **96**, 6796 (1992).
[30] R. Kobayashi, R. D. Amos, and N. C. Handy, J. Chem. Phys. **100**, 1375 (1994).
[31] C. D. Sherrill, A. I. Krylov, E. F. C. Byrd, and M. Head-Gordon, J. Chem. Phys. **109**, 4171 (1998).
[32] T. H. Dunning, Jr., J. Chem. Phys. **55**, 716 (1971).
[33] S. Huzinaga, J. Chem. Phys. **42**, 1293 (1965).
[34] R. Ditchfield, Mol. Phys. **27**, 789 (1974).
[35] J. Olsen and P. Jørgensen, J. Chem. Phys. **82**, 3235 (1985).
[36] P. Jørgensen, H. J. A. Jensen, and J. Olsen, J. Chem. Phys. **89**, 3654 (1988).
[37] O. Christiansen, A. Halkier, H. Koch, P. Jørgensen, and T. Helgaker, J. Chem. Phys. **108**, 2801 (1998).
[38] O. Christiansen, P. Jørgensen, and C. Hättig, Int. J. Quantum Chem. **68**, 1 (1998).
[39] T. Helgaker *et al.*, *Dalton, A Molecular Electronic Structure Program, release* 1.2.1, 2001.
[40] C. Angeli *et al.*, *Dalton, A Molecular Electronic Structure Program, release 2.0*, 2005.
[41] S. F. Mason and G. E. Tranter, Chem. Phys. Lett. **94**, 34 (1983).
[42] L. Wiesenfeld, Mol. Phys. **64**, 739 (1988).
[43] P. Lazzeretti and R. Zanasi, Chem. Phys. Lett. **279**, 349 (1997).
[44] A. Bakasov, T.-K. Ha, and M. Quack, J. Chem. Phys. **109**, 7263 (1998); A. Bakasov, T.-K. Ha, and M. Quack, *ibid.* **110**, 6081 (E) (1999).
[45] T. Kitayama, H. Kiyonaga, K. Morihashi, O. Takahashi, and O. Kikuchi, J. Mol. Struct. **589-590**, 183 (2002).
[46] A. D. Becke, Phys. Rev. A **38**, 3098 (1988).
[47] C. Lee, W. Yang, and R. G. Parr, Phys. Rev. B **37**, 785 (1988).
[48] A. C. Hennum, T. Helgaker, and W. Klopper, Chem. Phys. Lett. **354**, 274 (2002).
[49] P. Schwerdtfeger, T. Saue, J. N. P. van Stralen, and L. Visscher, Phys. Rev. A **71**, 012103 (2005).
[50] M. Schindler and W. Kutzelnigg, J. Chem. Phys. **76**, 1919 (1982).
[51] R. Bast, P. Schwerdtfeger, and T. Saue (unpublished).
[52] S. Nahrwold and R. Berger (work in progress).